Front. Electr. Electron. Eng. China 2009, 4(3): 330–334
DOI 10.1007/s11460-009-0054-6

RESEARCH ARTICLE

Chongqing JIAO

Preliminary design of 1 MW, Ku-band gyrotron traveling-wave amplifier

Abstract The preliminary design results of a 1-MW, Ku-band gyrotron traveling wave amplifier (gyro-TWA) are presented. Operating at the second cyclotron harmonic of the TE_{11} mode, the amplifier characterizes good stability even in the case of no distributed losses loaded, which could potentially allow it to be operated at high average power. Large signal simulation shows that the amplifier can generate a saturated peak power of about 1 MW with efficiency of 26.6%, gain of 31 dB, and 3-dB bandwidth of about 1 GHz when driven by a 100 kV, 40 A electron beam with 5% axial velocity spread.

Keywords gyrotron traveling wave amplifier (gyro-TWA), Ku-band, millimeter wave amplifier

1 Introduction

Based on the instability of electron cyclotron maser, gyrotron traveling wave amplifier (gyro-TWA) can generate high power and broad bandwidth coherent radiation in the millimeter and sub-millimeter wavelength ranges. Potential applications of gyro-TWA include high-density communications, advanced radar, high-gradient linear colliders, and atmospheric sensing. Steady progress in theory and experiment has been made over an extended period of time. Major advances in gyro-TWA performances have been reported in the review papers [1–3].

The primary obstacle to the development of gyro-TWA has been its susceptibility to spurious oscillations, such as absolute instability [4] and gyrotron backward-wave oscillator (gyro-BWO) [5]. In recent years, great efforts, primarily in the design of novel interaction circuit, have been made to improve the stability of gyro-TWA. Distributed wall losses configuration is efficient for suppressing spurious oscillations, but it is not usually appropriate for high average power operation [6,7]. Mode-selective circuits, such as slotted waveguide and helically corrugated waveguide [8–11], can also be used to improve the stability. However, the circuits are usually complicated in manufacturing and in coupling with input or output circuit of gyro-TWA.

In this paper, the preliminary design of a Ku-band, 1 MW gyrotron traveling wave tube (gyro-TWT) amplifier is presented. The amplifier is able to remain stable in spite of the high-power electron beam because it operates at the second harmonic of the lowest-order TE_{11} mode. The circuit is also capable of withstanding high average power because no distributed wall losses are required to achieve stability. Section 2 presents the stability of the proposed gyro-TWA. The predicted large-signal characteristics of the amplifier are described in Sect. 3, and a summary is given in Sect. 4.

2 Stability analysis

The amplifier design was developed by following the marginal stability design procedure [12]. Because a large axial velocity is beneficial for stability and wide bandwidth, the operating voltage of 100 kV and the velocity ratio of 1.0 are chosen. The interaction circuit is a circular waveguide with the radius of 5.3 mm, which means a cutoff frequency of 16.6 GHz for the lowest-order TE_{11} mode. The dispersion diagram for the second-harmonic TE_{11} mode amplifier is shown in Fig. 1. An important feature of the proposed amplifier is that there is no competing interaction at the fundamental harmonic ($s = 1$) because the fundamental cyclotron resonance line is well below the lowest order mode of waveguide. It can also be seen that, for the amplifier, the possible competing oscillations include TE_{11} mode absolute instability at the second cyclotron harmonic, TE_{11} mode gyro-BWO at the third cyclotron harmonic, and the TE_{21} mode gyro-BWO at the fourth cyclotron harmonic.

Received January 6, 2009; accepted March 23, 2009

Chongqing JIAO (✉)
Beijing Key Laboratory of High Voltage & EMC, North China Electric Power University, Beijing 102206, China
E-mail: cqjiao@ncepu.edu.cn

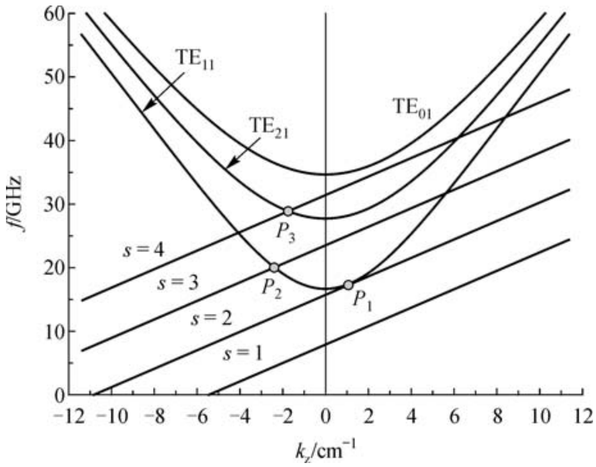

Fig. 1 Dispersion diagram of operating mode and possible oscillating modes (100 kV, $\alpha = 1.0$)

Figure 2 shows that the beam-wave coupling coefficient [13] increases with the increase of the electron beam's guiding-center radius for $TE_{11}^{(2)}$ operating mode and two gyro-BWO modes (superscript refers to the cyclotron harmonic number). Wherein, r_w and r_c are waveguide radius and electron guiding center radius, respectively. Therefore, larger guiding-center radius means stronger beam-wave coupling for the operating mode. However, in order to reduce the interaction strength of two oscillation modes and to reduce the interception of electron beam during passing interaction circuit, a value for r_c/r_w of 0.4 was chosen for design. Since the Larmor radii of electrons are 2.4 mm, there is no concern for the electron hitting the waveguide wall.

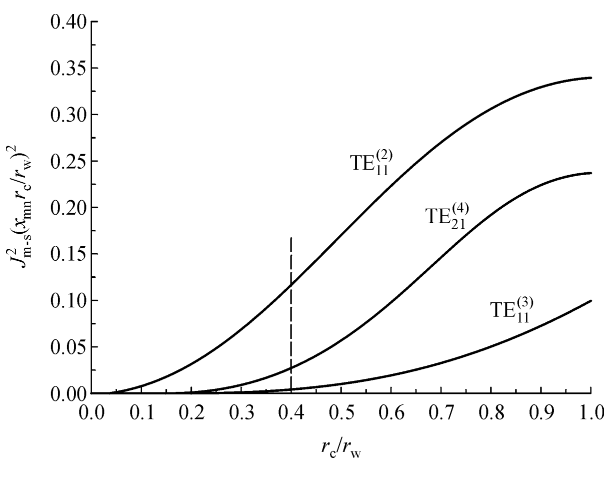

Fig. 2 Dependence of beam-wave coupling coefficient on guiding-center radius for operating mode and possible competing modes

Analytical linear theory has been used to determine the critical beam current for absolute instability. An absolute instability develops when the amplifier's operating bandwidth extends to cutoff frequency. A backward wave will then be excited from internal feedback. To ensure that the second-harmonic gyro-TWT amplifier is stable to the absolute instability of operating TE_{11} mode, operating electron beam current should be lower than the threshold value determined by using the analytic formula in Refs. [4,13]. Figure 3 shows the dependence of threshold value on applied magnetic field. Wherein, B_0 is applied magnetic field and B_g is "grazing" magnetic field [13]. V_b and α are voltage and velocity ratio of electron beam, respectively. It can be seen that the threshold current of absolute instability decreases with the increase of applied magnetic field. For a 100-kV electron beam with velocity ratio of 1.0, the threshold current is approximately 90 A at $B_0 = 0.99B_g$, which yields a wide safety margin for stability for designed operating beam current of 40 A.

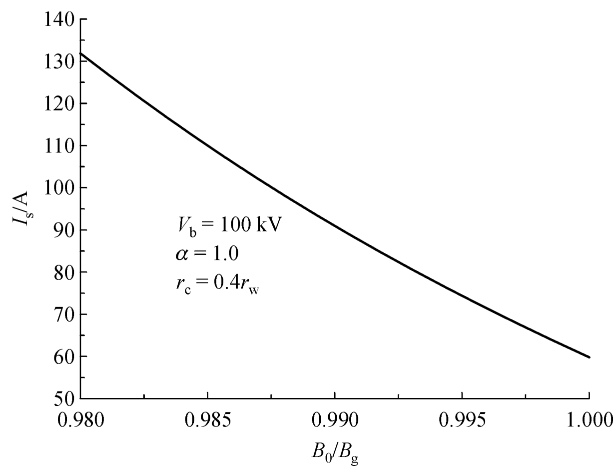

Fig. 3 Dependence on applied magnetic field of start-oscillation current for TE_{11} mode, second-harmonic absolute instability

A gyro-TWT amplifier is also susceptible to self-oscillation as a gyrotron backward-wave oscillator (gyro-BWO) at a harmonic of cyclotron frequency. This wave propagates counter to the direction of electron beam and therefore benefits from internal feedback. The amplifier's stability can be maintained, however, if interaction length is kept shorter than critical length for gyro-BWO oscillation to start. The linear theory could be used to determine the oscillation length [14] for the start of gyro-BWO in the second-harmonic TE gyro-TWT amplifier. Due to the weaker strength of the fourth cyclotron harmonic interaction, the $TE_{21}^{(4)}$ gyro-BWO is difficult to be excited. Meanwhile, the $TE_{11}^{(3)}$ gyro-BWO is also difficult to be excited because its operating point is far from its cutoff frequency as shown in Fig. 1. The underlying reason is that wave impedance of TE mode is proportional to $1/k_z$. With the increase of wave frequencies, k_z increases and hence wave impedance decreases, which can result in the weakening of beam-wave interaction strength. Figure 4 presents starting oscillation length and frequency for $TE_{11}^{(3)}$ gyro-BWO. It can be seen that critical length increases with the increase of applied magnetic field B_0. Meanwhile, starting oscillation frequency also increases in accordance with B_0, because it is approximately equal to the frequency corresponding to intersection point of straight line of "$s=3$" and hyperbolic curve of "TE_{11}" as shown in Fig. 1.

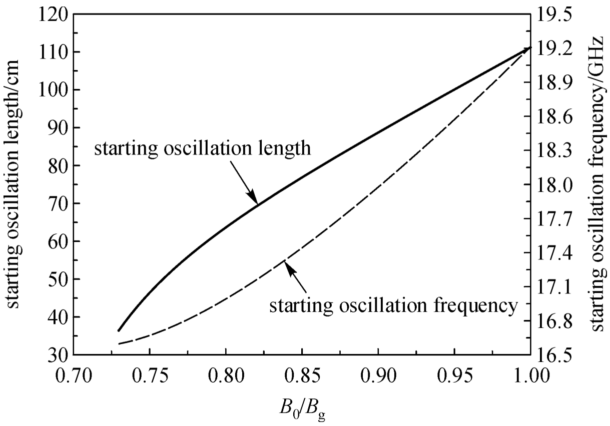

Fig. 4 Dependence on applied magnetic field of start-oscillation current and frequency for TE_{11} mode, third-harmonic gyro-BWO

Considering higher operating current, gyromonotron-type parasitic oscillation of TE_{11} mode may also be a threat to stable operation of the amplifier. In order to evaluate this possibility, the analytic formula in Ref. [15] is used to calculate starting current of oscillation, and the corresponding results are shown in Fig. 5, wherein, waveguide length and diffraction Q-factor of the open waveguide (Q_d) are assumed to be 60 cm and 30000, respectively. It can be seen from Fig. 5 that starting current is extremely sensitive to the value of applied magnetic field. At about B_0= 0.353 T, where two dispersion lines intersect near cutoff as shown in Fig. 6, the current reaches its minimum and the

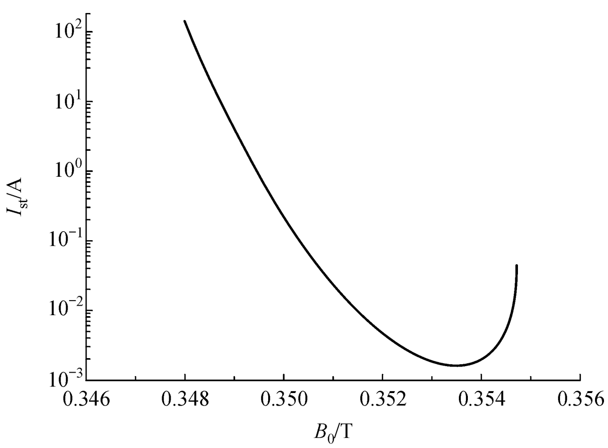

Fig. 5 Starting current of TE_{11} gyromonotron-type oscillation versus applied magnetic field with $L=60$ cm and Q_d= 30000

oscillation can be excited more easily. When $B_0 < 0.35$ T, the current increases sharply with the decrease of applied magnetic field, and starting current is above 100 A at B_0= 0.348 T. The underlying reason is that, with the decrease of B_0, the intersection moves away from cutoff to forward wave region as shown in Fig. 6. Especially, for design value of 0.323 T, two lines have no intersection and beam dispersion line is well below cutoff. Therefore, TE_{11} gyromonotron-type oscillation is difficult to be excited in the amplifier.

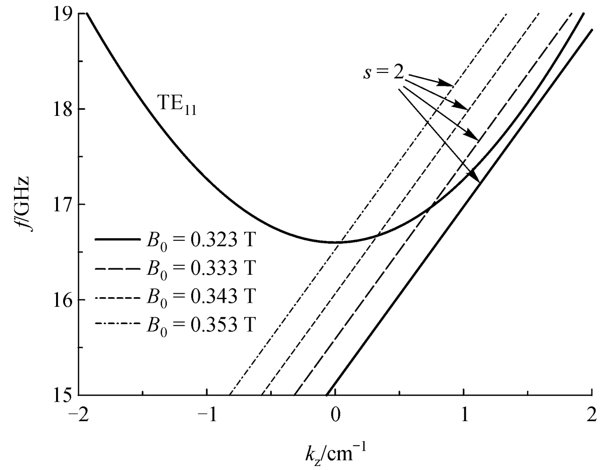

Fig. 6 Dispersion diagram of TE_{11} second-harmonic gyro-TWA for different values of applied magnetic field

3 Large signal simulations

Although linear theory is useful to find starting conditions for oscillation, large-signal theory is necessary to simulate nonlinear behavior and determine saturated efficiency. In this section, a large signal simulation code developed according to self-consistent nonlinear theory presented in Refs. [16,17] is used to study the large signal characteristics of gyro-TWA with the following operating parameters: 100 kV, 40 A, $\alpha=1.0$, $B_0=0.99B_g=0.323$ T and interaction circuit length of 60 cm. Magnetic field has been chosen so that the second-harmonic cyclotron resonance line nearly grazes TE_{11} waveguide mode. Although a grazing value of a magnetic field produces broadest bandwidth, a slightly detuned value yields higher efficiency. Chosen single-stage length of 60 cm is less than start-oscillation length for TE_{11} gyro-BWO with a 70% margin of safety. As a result, no distributed wall losses are needed for the gyro-TWA, which could potentially allow it to be operated at high average power.

The calculated saturated power, efficiency and gain are shown for different values of velocity spread in Fig. 7 and Fig. 8, respectively, where a Gaussian velocity distribution function is assumed. It can be seen that velocity spread can greatly deteriorate the performance of the amplifier in high-frequency region of the amplifier and hence narrow amplifier's bandwidth. The underlying reason is that the effect is in combination with Doppler broadening $k_z\Delta v_z$ qualitatively. At higher frequencies, k_z becomes sizable and the effect of velocity spread will then be important [18]. For axial velocity spread of 5%, predicted peak power is 1.06 MW at 16.95 GHz with an efficiency of 26.6% and a gain of 31 dB, predicted peak gain is 42.6 dB at 17.3 GHz with an output power of 0.72 MW, and 3-dB bandwidth of the amplifier is about 1 GHz (from 16.9 GHz to 17.9 GHz).

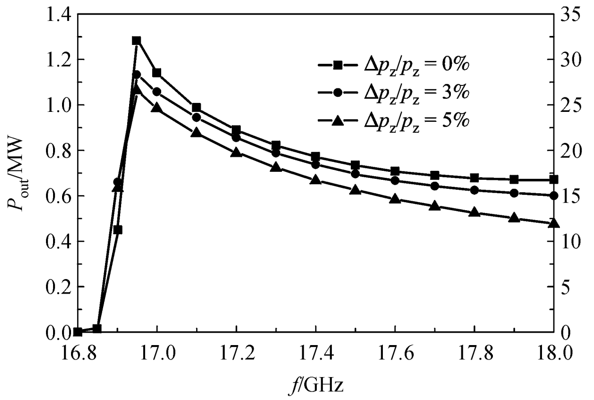

Fig. 7 Calculated saturated power and efficiency of amplifier for different values of velocity spread

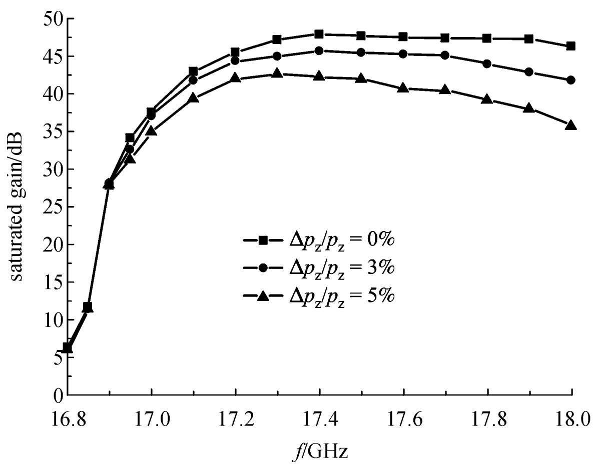

Fig. 8 Calculated saturated gain of amplifier for different values of velocity spread

4 Conclusions

The preliminary design of a 1-MW, TE_{11} mode, second-harmonic, Ku-band gyro-TWA has been carried out. Resulting from low-order operating mode and high cyclotron harmonic, the amplifier could operate stably and characterize low losses, high average power capability, and low magnetic field requirement. Driven by a 100 kV, 40 A electron beam with 5% axial velocity spread, the amplifier is predicted to generate saturated peak power of about 1 MW with an efficiency of 26.6%, gain of 31 dB, and 3-dB bandwidth of about 1 GHz.

Acknowledgements This work was supported by the Funds for Doctor Degree Teacher of North China Electric Power University (Grant No. 200822008).

References

1. Felch K L, Danly B G, Jory H R, Kreischer K E, Lawson W, Levush B, Temkin R J. Characteristics and applications of fast-wave gyrodevices. Proceedings of the IEEE, 1999, 87(5): 752–781
2. Chu K R. Overview of research on the gyrotron traveling-wave amplifier. IEEE Transactions on Plasma Science, 2002, 30(3): 903–908
3. Granatstein V L, Levush B, Danly B G, Parker R K. A quarter century of gyrotron research and development. IEEE Transactions on Plasma Science, 1997, 25(6): 1322–1335
4. Lau Y Y, Chu K R, Barnett L R, Granatstein V L. Gyrotron travelling wave amplifier: I. Analysis of oscillations. International Journal of Infrared and Millimeter Waves, 1981, 2(3): 373–393
5. Chu K R, Chen H Y, Hung C L, Chang T H, Barnett L R. Ultrahigh gain gyrotron traveling wave amplifier. Physical Review Letters, 1998, 81(21): 4760–4763
6. Garven M, Calame J P, Danly B G, Nguyen K T, Levush B, Wood F N, Pershing D E. A gyrotron-traveling-wave tube amplifier experiment with a ceramic loaded interaction region. IEEE Transactions on Plasma Science, 2002, 30(3): 885–893
7. Chu K R, Chen H Y, Hung C L, Chang T H, Barnett L R, Chen S H, Yang T T, Dialetis D J. Theory and experiment of ultrahigh-gain gyrotron traveling wave amplifier. IEEE Transactions on Plasma Science, 1999, 27(2): 391–404
8. Bratman V L, Cross A W, Denisov G G, He W, Phelps A D, Ronald K, Samsonov S V, Whyte C G, Young A R. High-gain wide-band gyrotron traveling-wave amplifier with a helically corrugated waveguide. Physical Review Letters, 2000, 84(12): 2746–2749
9. Wang Q S, McDermott D B, Luhmann N C Jr. Operation of a stable 200-kW second-harmonic gyro-TWT amplifier. IEEE Transactions on Plasma Science, 1996, 24(3): 700–706
10. Rodgers J, Guo H, Granaatstein V L, Chen S H, Nusinovich G S, Walter M, Zhao J. High efficiency, phase-locked operation of the harmonic-multiplying inverted gyrotwystron oscillator. IEEE Transactions on Plasma Science, 1999, 27(2): 412–421
11. Jiao C Q, Luo J R. Preliminary design of a harmonic-doubling gyrotron traveling wave amplifier. International Journal of Infrared and Millimeter Waves, 2007, 28(12): 1095–1101
12. Lin A T, Chu K R, Lin C C, Kou C S, McDermott D B, Luhmann N C Jr. Marginal stability design criterion for gyro-TWT's and comparison of fundamental with second harmonic operation. International Journal of Electronics, 1992, 72(5): 873–885
13. Chu K R, Lin A T. Gain and bandwidth of the gyro-TWT and CARM amplifiers. IEEE Transactions on Plasma Science, 1988, 16 (2): 90–104
14. Kou C S, Wang Q S, McDermott D B, Lin A T, Chin K R, Luhmann N C Jr. High-power harmonic gyro-TWT's. I. Linear theory and

oscillation study. IEEE Transactions on Plasma Science, 1992, 20 (3): 155–162
15. Danly B G, Temkin R J. Generalized nonlinear harmonic gyrotron theory. Physics of Fluids, 1986, 29(2): 561–567
16. Wang Q S, Kou C S, McDermott D B, Lin A T, Chu K R, Luhmann N C. High-power harmonic gyro-TWT's. II. Nonlinear theory and design. IEEE Transactions on Plasma Science, 1992, 20(3): 163–169
17. Jiao C Q, Luo J R. Linear and nonlinear analysis of a gyrotron traveling wave amplifier with misaligned electron beam. Physics of Plasmas, 2006, 13(11): 113101-1–113101-7
18. Lau Y Y, Chu K R, Barnett L, Granatstein V L. Gyrotron travelling wave amplifier: II. Effects of velocity spread and wall resistivity. International Journal of Infrared and Millimeter Waves, 1981, 2(3): 395–413